

# Chapter 5

---

**Organic homo-junction based thin  
film transistor for ammonia sensing  
applications**

---

**Abstract**

An extremely sensitive ammonia (NH<sub>3</sub>) sensor was developed using an aligned nanowires/thin film hybrid channel of an organic thin film transistor (OTFT). Conjugated polymer poly(2,5-bis(3-tetradecylthiophen-2-yl)thieno(3,2-b)thiophene) (PBTFT-C14) has been used as semiconductor channel that has been fabricated via 'floating film transfer method' (FTM). The crystalline fibrillar microstructure within the liquid phase of the polymer has been developed by mixed solvent, which has been self-assembled on the air-liquid interface through the FTM method. This hybrid structured film was then transferred on a cleaned Si/SiO<sub>2</sub> substrate, whereas Au was used as source-drain electrodes of this OTFT. To investigate the ammonia sensing behavior of the designed OTFT, various low concentrations of the NH<sub>3</sub> have been exposed on the channel ranging from 0.2 ppm to 5 ppm. From the accumulation mode drain current variation, it was observed that the sensor is extremely sensitive towards ammonia gas with a response of about 75% at 5 ppm, whereas the limit of detection (LOD) is ~0.67 ppm, which confirms its applicability at the lower concentrations. More interestingly, the depletion mode current of this OTFT reduces ~ 200 times during this investigation, which is ~40 times larger variation than accumulation mode current. Additionally, these current variations of this sensor have excellent linearity to NH<sub>3</sub> concentration. This fabricated sensor also exhibits excellent selectivity and sensitivity to NH<sub>3</sub> gas, which can satisfy requirements for real-world applications.

**5.1. Introduction**

Chemical gas sensors have gain significant interest due to their widespread applications in modern civilization. Electrical gas sensors can be fabricated using different inorganic nano-structured materials, organic/polymer based semiconductor, carbon nano-structured based materials etc.[164-166]. Among different materials organic semiconductor (OS) based chemical

sensors are getting more attention because of their considerable variety in molecular design, high sensitivity with excellent selectivity at ambient conditions [167-170]. However, pure conducting polymer based sensors acquire low sensitivity towards analyte gases. Earlier, different nanostructures OS and organic/inorganic hybrid nanostructure have been used to improve the sensitivity of gas sensors [161, 171]. Owing to the noticeable structure, several techniques have been devised to modify the OS nanostructures in order to investigate the links between nanostructure to the enchantment of gas sensitivity [83, 172]. Besides, device geometry also plays a key role to improve its sensitivity and reliability. Among them the utilization of organic thin film transistors (OTFTs) as gas sensors has received considerable interest due to its advantages like higher sensitivity, option of direct interaction of semiconductor channel with analyte, functioning at room temperature etc. [169, 173-175]. In order to enhance the sensor's overall performance, it is imperative to exert control over the morphology by inducing in-plane ordering within the polymer [168, 176]. Several procedures have been utilized to achieve long-range ordering of polymer chains, including vaporization induced self-assembly, poor solvent induced assembly, ageing, high temperature rubbing, lithography, electro-spinning, and epitaxial crystallization [56, 58, 177-180]. Among them, poor solvent induced ageing is an economically viable method that synthesizes long fibers and could be an ideal choice for low cost and large area fabrication [181, 182]. In a mixture of good and poor solvent of a polymer, the poor solvent component generates collapsed coils of the polymer chains that work as a driving force for the self-assembly of polymers [183-185].

Among different gas sensors, ammonia (NH<sub>3</sub>) sensor is widely used, particularly for unavoidable exposure of different workplaces including industry, hospital, cold storage etc. Workplace NH<sub>3</sub> exposure has been set by the US Occupational Safety and Health Administration (OSHA) at 50

ppm for eight hours a day, 25 ppm for ten hours a day, and 40 ppm per week. For instance, the breath  $\text{NH}_3$  content may be several hundred parts per billion higher than normal in a patient with liver disease or urea balance issues [174, 186]. Commercialization hence necessitates an inexpensive and extremely sensitive  $\text{NH}_3$  gas sensitive system which operates at room-temperature [187, 188].

In this chapter, I am presenting an OTFT based  $\text{NH}_3$  gas sensor fabrication that has an aligned nano-wires/thin film hybrid morphology of PBTTT-C14 polymer channel. This PBTTT-C14 polymer has been used widely as  $\text{NH}_3$  gas sensor due to their higher air stability and high carrier mobility [156, 189]. A good-poor mixed solvent has been used to dissolve the PBTTT-C14 polymer that produces a fractional part of the film by crystalline fibrillar polymer nano-wire, which effectively forms this hybrid layer. A facial method called floating film transfer method (FTM) has been used to deposit this polymer channel. To investigate the room temperature  $\text{NH}_3$  sensing behavior of this gas sensor, the channel of the OTFT was exposed with ranges of concentrations of the ammonia from 0.2 ppm to 5 ppm and recorded the change in the OTFT parameters for the investigation of the sensitivity, selectivity and other important parameters.

## **5.2. Experimental methods**

### **5.2.1. Materials**

Conjugated polymer, PBTTT-C14 with a molecular weight of more than 40,000 is acquired from Sigma-Aldrich, India. Both analytical-grade chloroform and toluene were attained from Merck, India.

### 5.2.2. Preparation of fibrillar PBTTT-C14 nanowires

By using the conception of solvent driven self-assembly of the polymer, PBTTT-C14 solution was prepared by the ageing of polymer dissolved in a pair of solvents of chloroform and toluene. In self-assembly of the polymer, pair solvent of chloroform and toluene were used as the good and poor solvents, respectively. For this procedure firstly, the mixed solvent volume ratio of chloroform and toluene has been taken 9:1 and then subsequently added with 5 mg/ml polymer concentration in a glass vial. This mixed polymer solution was then stirred on a magnetic hot plate at an elevated temperature of 90°C for 2 hours in a sealed glass vial for the complete dissolution. The heated solution was then left in closed chamber for 10 min allowing for the self-assembly of the polymer to form the nano-wires [182].

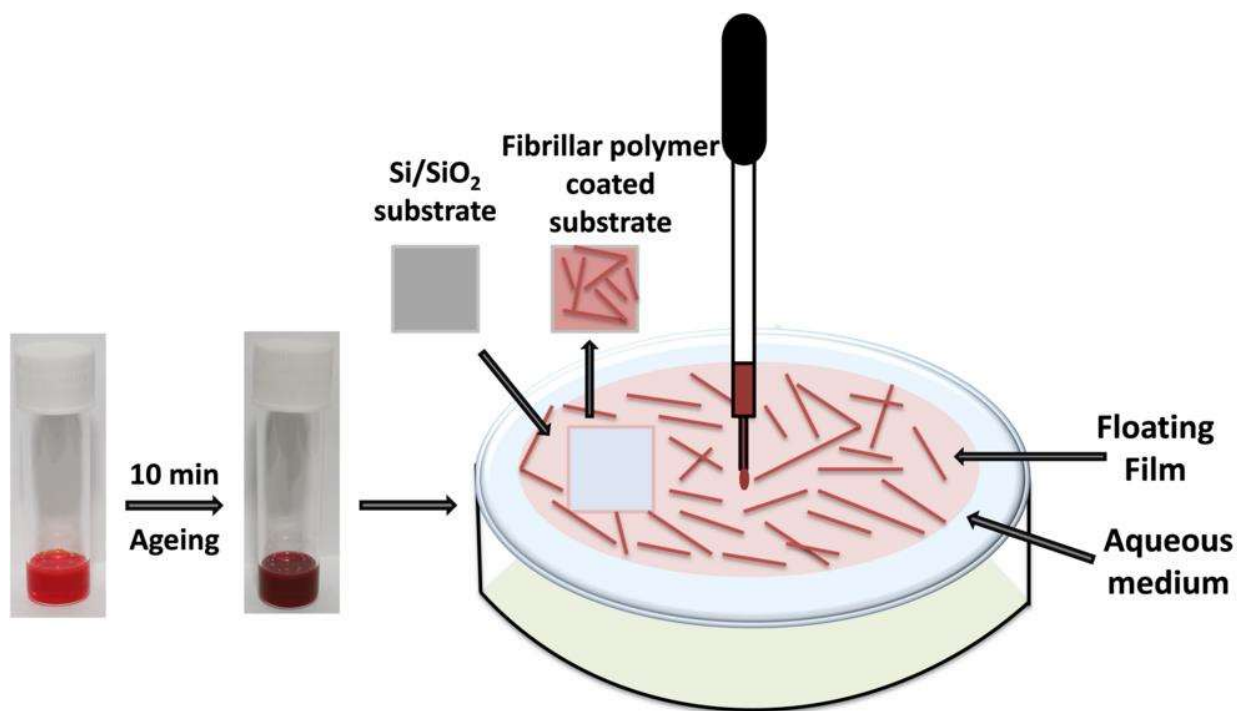


**Fig .5.1.** Demonstration of the self-assembly of the polymer and FTM method for the thin film fabrication.

In this mixed solvent, chloroform encourages polymer chain extension due to its high solubility, which enhances chain organization freedom and poor solvent creates unfavorable interactions with polymer chains, resulting in a driving factor for polymer self-assembly. Fig. 5.1 demonstrates as well-dissolved PBTBT ages, it creates fibers as it interacts with solvent molecules, and one prominent physical change that can be seen is the color changing from bright orange to dark brownish-purple as it goes through this transition. That aged solution has been used for thin film deposition via FTM method as shown in Fig .5.1. In which long-fibrous nano-wire polymer film is stamped onto the desired substrate for the sensing device fabrication.

### **5.2.3. Device fabrication**

For the bottom contact top gated OTFT based sensor fabrication, commercially available highly doped p<sup>++</sup> silicon substrates with a thermally grown SiO<sub>2</sub> (300 nm) layer are used as the gate dielectric. Initially, Si/SiO<sub>2</sub> substrates are thoroughly cleaned in an ultrasonic bath cleaner using distinct solvents: soap solution, deionized water, acetone, and isopropanol, and then dried at 80°C under nitrogen atmosphere. For the casting of the semiconducting/sensing layer on the cleaned substrate pre-described FTM method has been used, in which approximately 10 µl of the polymer solution was poured at the middle of a 10 cm diameter petri-dish containing hydrophilic liquid substrate (ethylene glycol and glycerol in a 3:1 ratio) under ambient conditions. In order to fabricate the OTFT, the formed polymeric fibrillar film over the liquid substrate was casted to the specified substrate as illustrated in Fig. 5.1, and dried in a nitrogen environment at 90°C. After that, a thermal vacuum evaporation unit with an interdigitated Ni shadow mask was used to construct source-drain electrodes of gold (Au) on top of a substrate covered with a semiconducting layer. The evaporation rate was 1.5 Å/s at vacuum 6×10<sup>-5</sup> Torr. The

interdigitated channels were 50  $\mu\text{m}$  in length and 18  $\mu\text{m}$  in width, respectively. Semiconductor device analyzer was used to measure the electronic properties of the fabricated device.

#### **5.2.4. Characterization**

To obtain the absorption spectra of the FTM coated PBTTT-C14 and fibrillar PBTTT nano-wire based film, UV–Vis spectrophotometer (UV-2600, Shimadzu) was used. X-ray diffractometer (Rigaku) is used for the crystallinity analysis of the films. The TEM micrographs with selected area electron diffraction (SAED) patterns of the fibrillar polymer film over Cu grid were obtained via TECHNAI G<sup>2</sup>20 TWIN (New Zealand). The roughness analysis of the film deposited substrate was performed by Atomic force micrograph (AFM) using NT-MDT “NTEGRA Prima” (Russia). Lastly, a controlled atmosphere gas sensing assembly was used to investigate the ammonia sensing performances of the OTFT sensor. There are two inlets and one outlet in the gas assembly. The first inlet is for injecting  $\text{NH}_3$  gas with the mass flow controller, while the second inlet and exit are for flushing air into and out of the chamber. A set of probes inside the test chamber are placed to connect devices with Keysight B1500A semiconductor parameter analyzer for their electrical characterization. Different concentrations of  $\text{NH}_3$  gas are passed through the inlet line of the test chamber under ambient temperature (temperature  $\sim 25^\circ\text{C}$  with RH of  $\sim 50\%$ ) with a regulated flow of dry air, and variation of electrical signal are observed using a parameter analyzer.

---

### 5.3. Results and discussion

#### 5.3.1. Optical and structural characterizations of PBTTT-C14 nano-wire thin film

As mentioned earlier, the color of mixed solvent PBTTT-C14 polymer solution changes over the time from bright orange to dark brownish-purple as it performs this transition. The detailed kinetics of the variation of absorption w.r.t time has been discussed in earlier report [182]. Simultaneously, the viscosity of the solution also increases along with the fiber synthesis process. Changes in color and viscosity are correlated with the numbers of non-dissolved microfibers present in the polymer solution. Specifically, the development of optical absorption of the polymer solution serves as a direct indicator of the degree of  $\pi$ - $\pi$  inter-chain contact, which is the driving force behind the production of nano-wires. The normalized absorption spectra of PBTTT-C14 films produced by FTM methods are shown in Fig 5.2(b). Both PBTTT-C14 films have single broad absorption band in their UV-vis spectra, which is typically present in polythiophene derivatives. The fibrillar PBTTT-C14 nano-wire film exhibits a more noticeable red-shift in its UV-vis spectrum, and its absorbance is higher than that of the isolated one. The higher energy absorption band (549 nm) appeared in both the cases due to  $\pi$ - $\pi^*$  transition. However, as the thiophene ring aged, an extra shoulder peak at lower energy 577 nm and 603 nm was observed as a result of the coupling of the  $\pi$ - $\pi^*$  transition to the C=C, as was also noted for P3HT.[190-192] Additional evidence for the molecular packing of PBTTT-C14 nano-wire films was investigated by XRD study (Fig. 5.2(c)). The diffraction peaks at 4.09, 8.30 and 12.42 are the results of the d-spacing (lamellar structure) of their crystal structure, which corresponds to the (100), (200) and (300) planes, respectively, indicating their structure towards

face-on orientation. These peaks moved toward higher  $2\theta$  values (that is, from 4.09 to 4.23 for (100) plane, from 8.30 to 8.42 for (200) plane and, from 12.29 to 12.56 for (300) plane), in comparison to its isolated akin. This behavior could be the consequence of face-on orientation leading to a decrease in d-spacing.

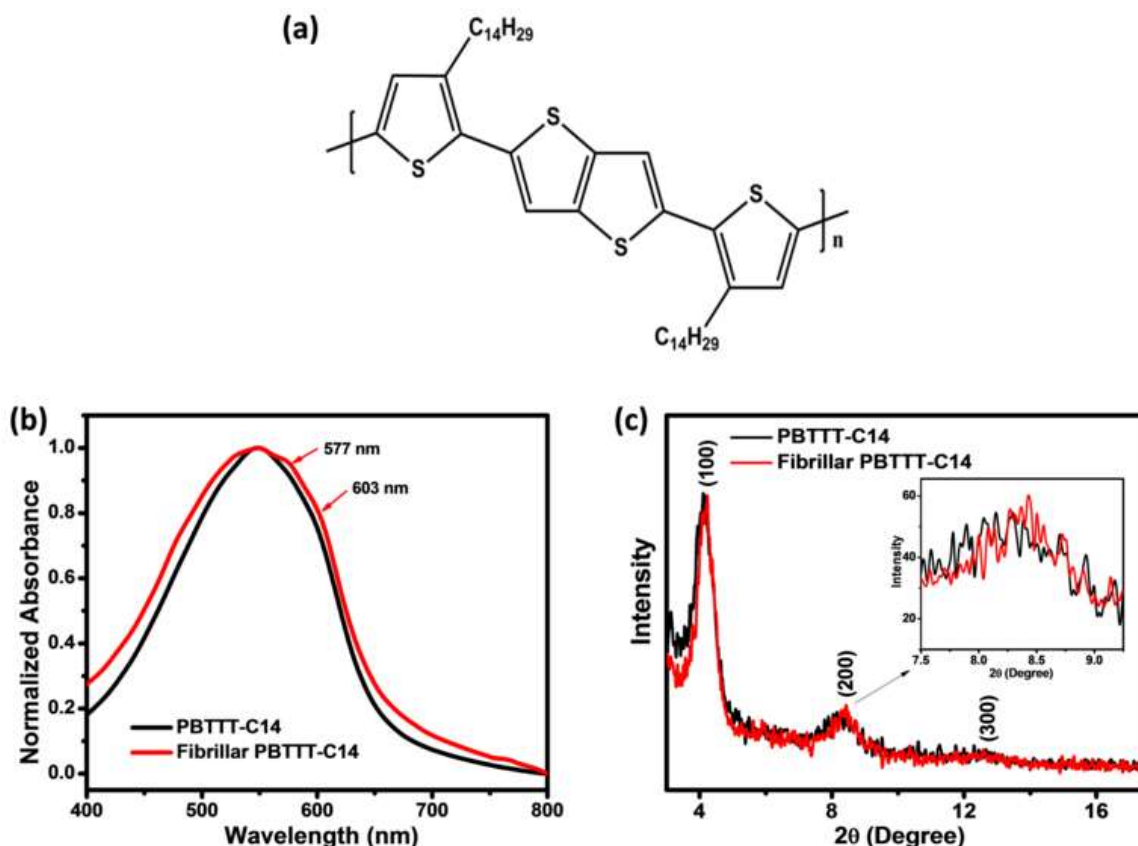


**Fig. 5.2.** (a) Chemical structure of PBTTT-C14, (b) UV-Vis spectroscopy of pristine and nano-wires/thin film hybrid PBTTT-C14 thin film, and (c) XRD pattern of pristine and nano-wires/thin film hybrid PBTTT-C14 (inset shows zoom view of (200) peak).

For the structural analysis of FTM coated fibrillar polymeric film, TEM analysis has been done by transferring the film via FTM method onto a carbon coated TEM grid. The TEM micrograph and SAED pattern of this polymer film is presented in Fig. 5.3(a) and 5.3(b), respectively. This

TEM micrograph clearly shows the aligned nano-wire formation over the area that is spread uniformly. Additionally, development of the SAED pattern indicates the nano-wires are crystalline in nature.

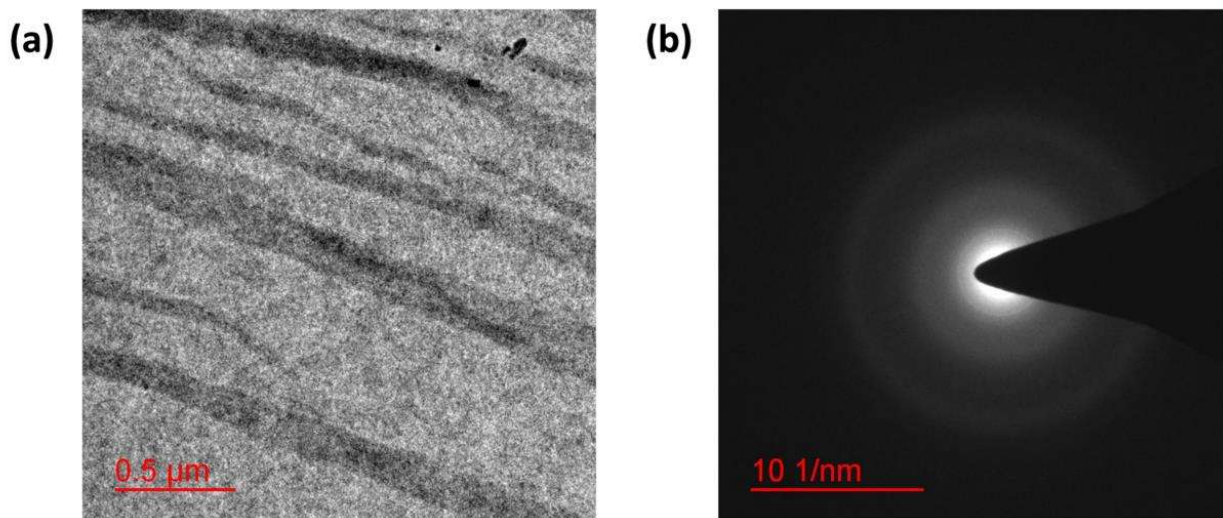


**Fig. 5.3.** (a) TEM image and, (b) SAED pattern of FTM coated PBTTT-C14 nanowire/thin film.

AFM characterization has been done by scanning 10 μm x 10 μm and 3 μm x 3 μm film regions, as illustrated in Fig. 5.4(a) and 5.4(b), which revealed the formation of polymeric fibrillar morphology consist of regular network of interconnected 1D nano-wires. The uniformity and self-alignment of these nano-wires are clearly visible in the micrographs. Fig. 5.4(c) shows the 3D structure that provides the regular height variation of the film due to this nano-wire formation, whereas Fig. 5.4(d) shows the height profile of the nano-wire, indicating its diameter and height are ~ 300 nm and 20 nm respectively. From careful AFM studies of different parts of the film, we measured the average coverage of such nano-wire in the film with the help of image J. This study indicates the nano-wire is covering ~26% of the film area.

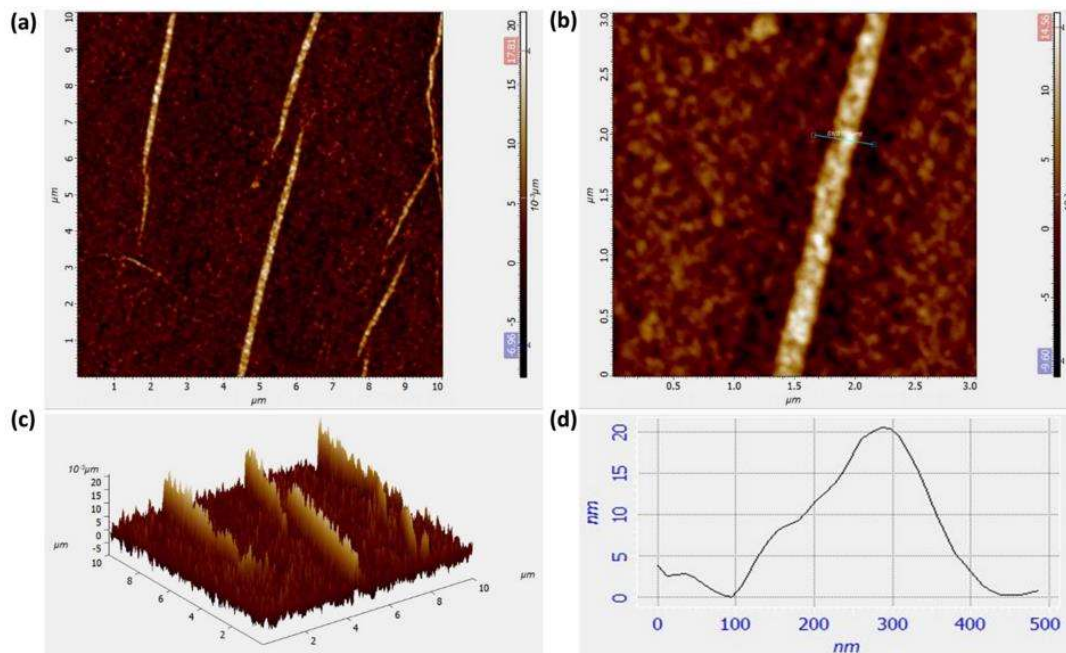


**Fig. 5.4.** (a), (b) AFM images of the FTM coated fibrillar PBTTT-C14 and, (c) corresponding 3D image and (d) AFM height profile of the film.

### 5.3.2. Electrical Characterization

Figure 5.5 illustrates the ambient condition (25°C with 50% RH) electrical characterization (current-voltage characteristics) of the designed top contact bottom gated transistor. The output ( $I_{DS}$ - $V_{DS}$ ) characteristics of the PBTTT-C14 nano-wire/thin film hybrid channel based OTFT are shown in Fig. 5.5(a). During this study, the drain voltage has been swept in the range of 0 to -30 V with various constant gate biases. Fig. 5.5(b) shows the transfer ( $I_{DS}$ - $V_{GS}$ ) characteristics in which gate bias has been varied from 0 to -30 V and keeping drain bias at -30 V. Important transistor electrical parameters, like mobility ( $\mu_h$ ) and threshold voltage ( $V_{TH}$ ), are derived from transfer characteristics by using the equation (3.1). The fitted straight line that corresponds to the

$I_{DS}^{1/2}$  against  $V_{GS}$  curve at  $V_{DS} = -30$  V is extrapolated to find the threshold voltage of the designed OTFT.

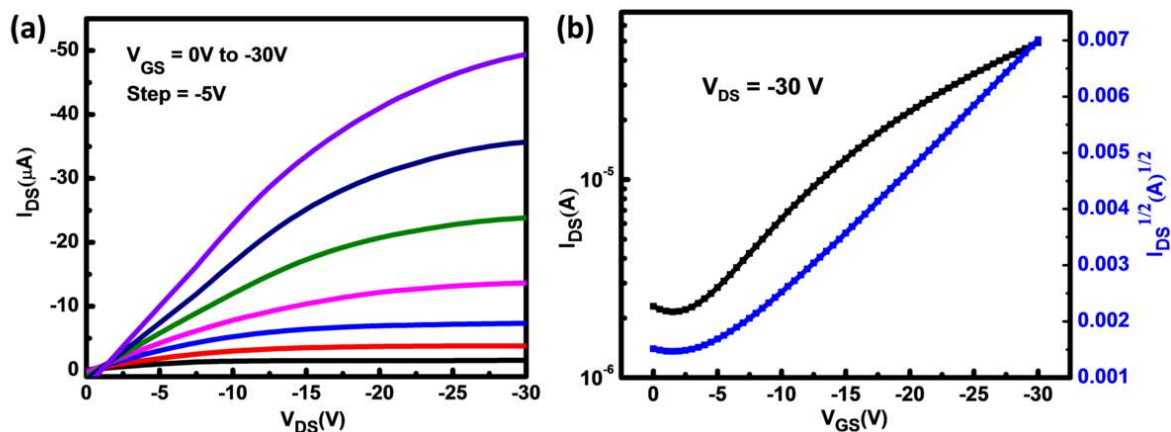


**Fig. 5.5.** (a) Output characteristics, and (b) Transfer characteristics of PBTTC-C14 nanowire/thin film hybrid channel OTFT.

### 5.3.3. Ammonia sensing analysis

For the purpose of  $NH_3$  sensing analysis, OTFT channel is exposed to different concentrations of  $NH_3$  gas, ranging from 0 ppm to 5 ppm, at  $25^\circ C$  under the regulated flow of dry air inside a sealed container with 50% relative humidity, as seen in Fig. 5.6(a). The gate bias ( $V_{GS}$ ) is swept from 0 to -30 V throughout the sensing measurement, while the drain voltage ( $V_{DS}$ ) is fixed to -30 V. The transfer characteristic shows that the drain current ( $I_{DS}$ ) of the OTFT steadily drops as soon as the  $NH_3$  concentration rises and almost saturates after being exposed to more than 5 ppm  $NH_3$  gas concentration.

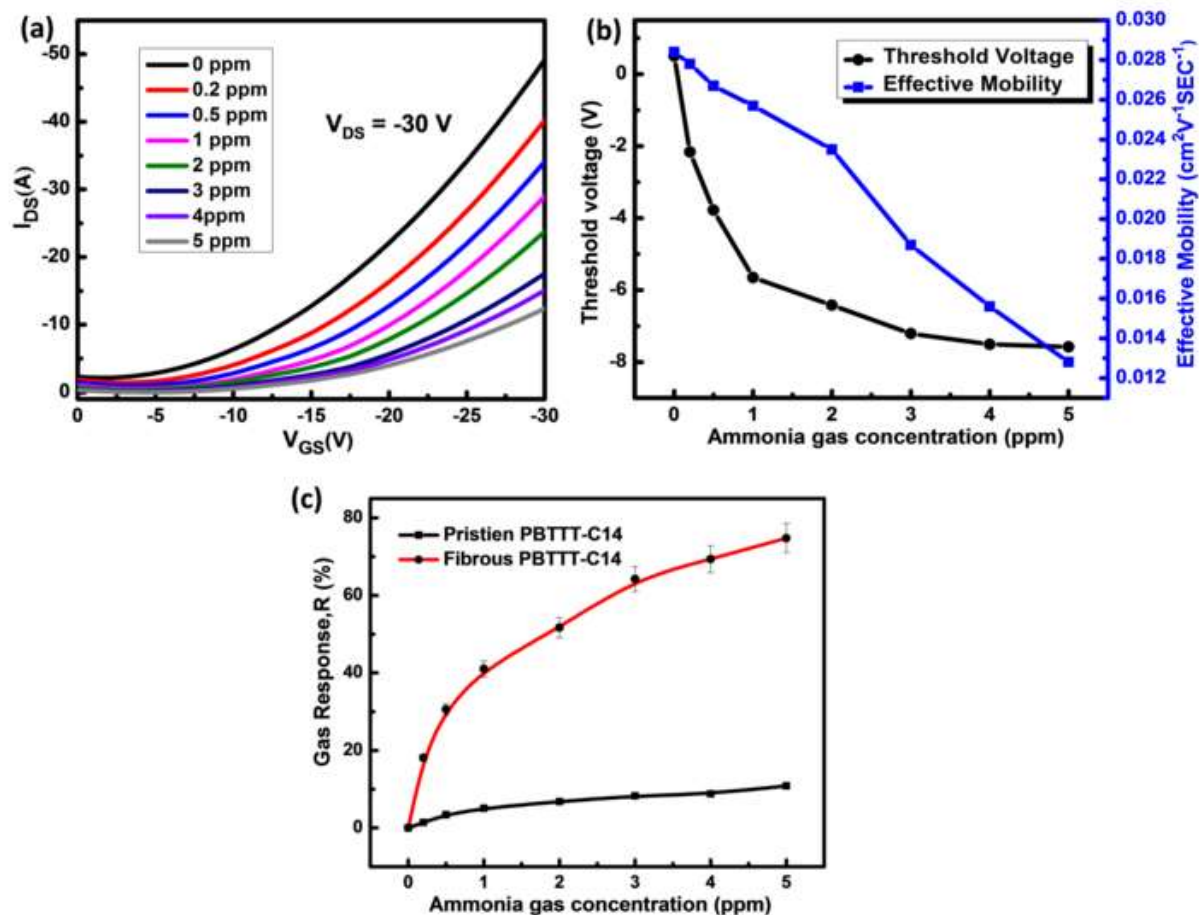


**Fig. 5.6.** (a) Transfer characteristics of PBTTT-C14 nano-wire/thin film hybrid channel OTFT sensor at  $V_{DS} = -30$  V, and (b) Corresponding Shift in threshold voltage ( $V_{TH}$ ) and mobility ( $\mu_h$ ) with different concentrations of ammonia (0 ppm-5 ppm), (c) Gas response graph of the fabricated OTFT sensor at  $V_{DS} = -30$  V (The data points with black line indicates the response of pristine PBTTT-C14 based OTFT device).

The decrease in drain current ( $I_{DS}$ ) of the OTFT is associated with the reduction of effective carrier mobility ( $\mu_h$ ) and threshold voltage shifting ( $V_{TH}$ ), which is due to the depletion of the channel caused by the  $\text{NH}_3$  molecules. This depletion forms a layer of static charge in the

channel that reduces effective carrier density of the channel resulting in the reduction of the accumulation mode current. Besides, due to the addition of a static depleted layer (positive charge) on top of the channel,  $V_{TH}$  of OTFT shifted towards a more negative direction. The variation in  $V_{TH}$  and  $\mu_h$  of the devices as a function of  $NH_3$  concentration is depicted in Fig. 5.6(b). The results demonstrate that there is a change of  $V_{TH}$  of more than 8 V during the exposure of various  $NH_3$  concentrations, with high linearity up to 5 ppm. Additionally, the designed sensor's effective carrier mobility also decreases from 0.0284 to 0.0128  $cm^2 V^{-1}sec^{-1}$ , which is about 50% of its initial value. We performed this  $NH_3$  sensing study several times with the same device and found  $\sim\pm 2\%$  variation of device parameters of these listed values. The reduction of accumulation mode drain current is used to determine the response (R) of the device. This R is defined from the ratio of variation of drain current with respect to the original drain current as shown in the equation (3.2).

The response (sensitivity) of the PBTTC-C14 nano-wire/thin film hybrid channel OTFT at 5 ppm concentration of  $NH_3$  is 74.8% (Fig. 5.6(c)), which is calculated at the constant value of  $V_{DS} = -30$  V corresponding to the Fig. 5.6(a). It can be noted that the response of this device is  $\sim 8$  times higher than the pristine PBTTC-C14 based OTFT (Fig. 5.6(c)). The limit of detection of the sensor was also estimated with the help of the following equation (3.3). The calculated LOD of the fabricated ammonia sensor is 0.67 ppm. It can be noted that the sensor exhibits a very acceptable response ( $\sim 18\%$ ) even at the concentration of 0.2 ppm. The variation in  $V_{TH}$  and  $\mu_h$  of the devices with various concentrations of ammonia gas is listed in Table-5.1

Table- 5.1: Variation in OTFT parameters and the sensitivity of the sensor with different concentrations of NH<sub>3</sub> gas.

NH <sub>3</sub> (ppm)	On current Ion (μA)	Effective Mobility μ <sub>h</sub> (cm <sup>2</sup> V <sup>-1</sup> sec <sup>-1</sup> ) x10 <sup>-2</sup>	Threshold voltage V <sub>th</sub> (V)	Change in Threshold voltage (ΔV <sub>th</sub> )	Response (%)
0	49.14	2.84	0.5	0	0
0.2	40.24	2.76	-2.16	2.66	18.11
0.5	34.10	2.67	-3.78	4.28	30.59
1	28.97	2.57	-5.65	6.15	41.03
2	23.75	2.35	-6.42	6.92	51.67
3	17.56	1.87	-7.21	7.21	64.26
4	15.05	1.56	-7.51	8.01	69.36
5	12.38	1.28	-7.58	8.08	74.80

It can be noted that as an NH<sub>3</sub> gas sensor, this fibrillar conjugated polymer based OTFT sensor provides various advantages such as room temperature operation with high sensitivity, rapid response to low-concentration analyte with the excellent selectivity to the NH<sub>3</sub> gas. Besides, this OTFT based sensor also offers both depletion and accumulation mode of operations, in which the variation of channel current is quite linear with NH<sub>3</sub> concentration, which is an important factor for practical application. Also, the manufacturing method of the sensor is pretty simple, which doesn't require any additional instrument for the NH<sub>3</sub> sensitive fibrillar polymer film fabrication. A comparative performance of the NH<sub>3</sub> sensor w.r.t the earlier reports are given in the Table-5.2.

Table-5.2: Comparative performance of the NH<sub>3</sub> sensor w.r.t the earlier reports.

Device Type	Sensing material	Deposition technique	Operating Temp.	Response (%)	Remark
Chemi-resistive	PANI/TiO <sub>2</sub>	chemical polymerization	RT	5.6% (117 ppm)	Poor response [193]
MSM	PDI-HIS	Drop casting	RT	35% (100 ppm)	Less Detection limit [128]
OTFT	P3HT	Spin coating	RT	100% (30 ppm)	High response time [194]
OTFT	PBTTT/Mo S <sub>2</sub> -QDs	FTM	RT	Accumulation Mode res.- 35.1% (5 ppm), depletion mode Off current factor- ~3.9	Slower recovery time/ not that sensitive for lower conc. [156]
OTFT	PBTTT/W S <sub>2</sub> -QDs	FTM	RT	Accumulation mode res. – 44.5% (5 ppm), depletion mode Off current factor- ~28	Quite good for high detection limit, and low concentration NH <sub>3</sub> detection [195]
OTFT (This work)	PBTTT Nano-wire	FTM	RT	Accumulation mode res.- 74.8% (5 ppm), depletion mode Off current factor - ~10 <sup>2</sup>	High sensing response at lower conc. in both operating modes (this work)

**5.3.4. Selectivity and Transient analysis**

To identify the selectivity of this sensor, the electrical characterization of this OTFT was tested with other interfering gases such as methane ( $\text{CH}_4$ ), propane ( $\text{C}_3\text{H}_8$ ), carbon dioxide ( $\text{CO}_2$ ), carbon monoxide ( $\text{CO}$ ). The relative response of OTFT in presence of those gases w.r.t the  $\text{NH}_3$  gas is presented in Fig. 5.7(a). It can be noted the response of the device at 5 ppm  $\text{NH}_3$  is several orders higher than that of 20 ppm other interfering gases. These findings imply that the PBTTT-C14 nano-wire/thin film hybrid channel OTFT sensor exhibits notable improvements in selectivity, indicating its considerable potential for use in low-cost, portable ammonia sensors. The level of response difference of interfering gases that we achieve in this work is quite higher w.r.t most of those reports.

To investigate the transient performance of the fabricated sensor, various concentrations of the ammonia have been exposed ranging from 1-5 ppm, on the OTFT channel. A step-wise trend has been obtained with the variation in drain current of the OTFT sensor, as depicted in Fig. 5.7(b). The fabricated sensor follows the physisorption mechanism dominantly, and acquires a rapid response time of 2 sec. However, the recovery time of the sensor is  $\sim 12$  sec which could be due to the slow desorption of  $\text{NH}_3$  from the channel. Further, it can be reduced by reducing the channel length. Besides, in a fixed concentration of analyte, we tested  $\sim 10$  successive cycles for its response behavior study that show quite repeatable cyclic behavior. However, above this range, the variation of  $I_{\text{DS}}$  slowly decays. After leaving this device for several hours, it works like a fresh device again. This type of fatigue behavior is very common for conducting polymer based sensors.

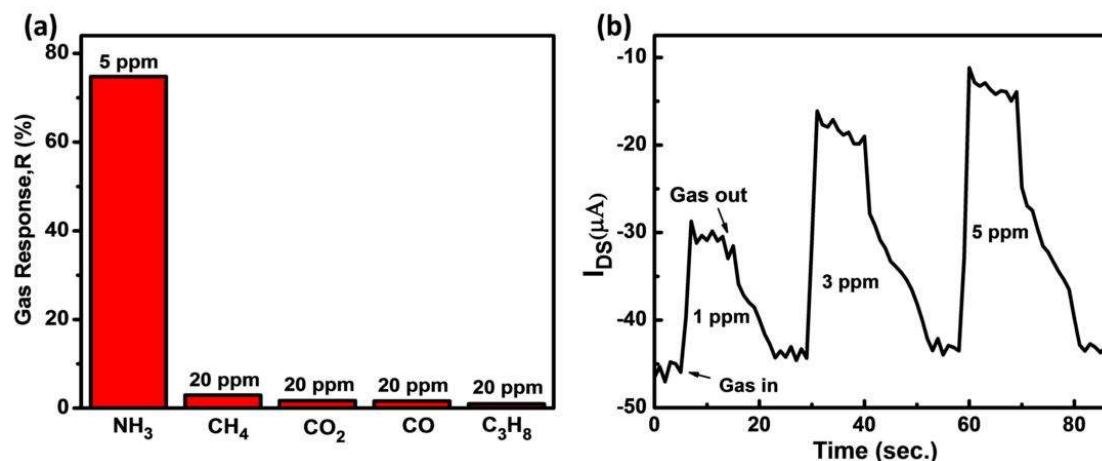


**Fig.5.7.** (a) Selectivity analysis, and (b) transient response of the OTFT sensor ( $V_{DS} = -30$  V, and  $V_{GS} = -30$  V).

### 5.3.5. Sensing mechanism

The variation of  $I_{DS}$  of this device in presence of analyte gas is primarily due to the reversible chemisorption or redox reaction. The organic PBTTT semiconductor is a p-type semiconductor and has provision to oxidize  $NH_3$  by sharing  $H^+$ . During the exposure of  $NH_3$  gas to the semiconductor channel, PBTTT is donating  $H^+$  through chemisorption ( $NH_3 + H^+ \leftrightarrow NH_4^+$ ), which is reversible phenomena. Besides, the preceding technique was designed to achieve a high  $NH_3$  sensing performance through the polymeric fibrillar nano-wire/thin film hybrid morphology for its higher specific surface area, which offers additional active sites for the ammonia molecule interactions (Figure 5.8(a)). These fibrillar morphologies are quite thick and have significantly high conductivity w.r.t the pristine PBTTT-C14 film, which decreases the sheet resistance of the OTFT channel very extensively. As a consequence, the ambient condition off current ( $\sim 2.15 \mu A$ ) of this aligned nano-wires/thin film hybrid channel based OTFT is  $\sim 2$  orders higher w.r.t the pristine film OTFT ( $\sim 0.68 \mu A$ ).

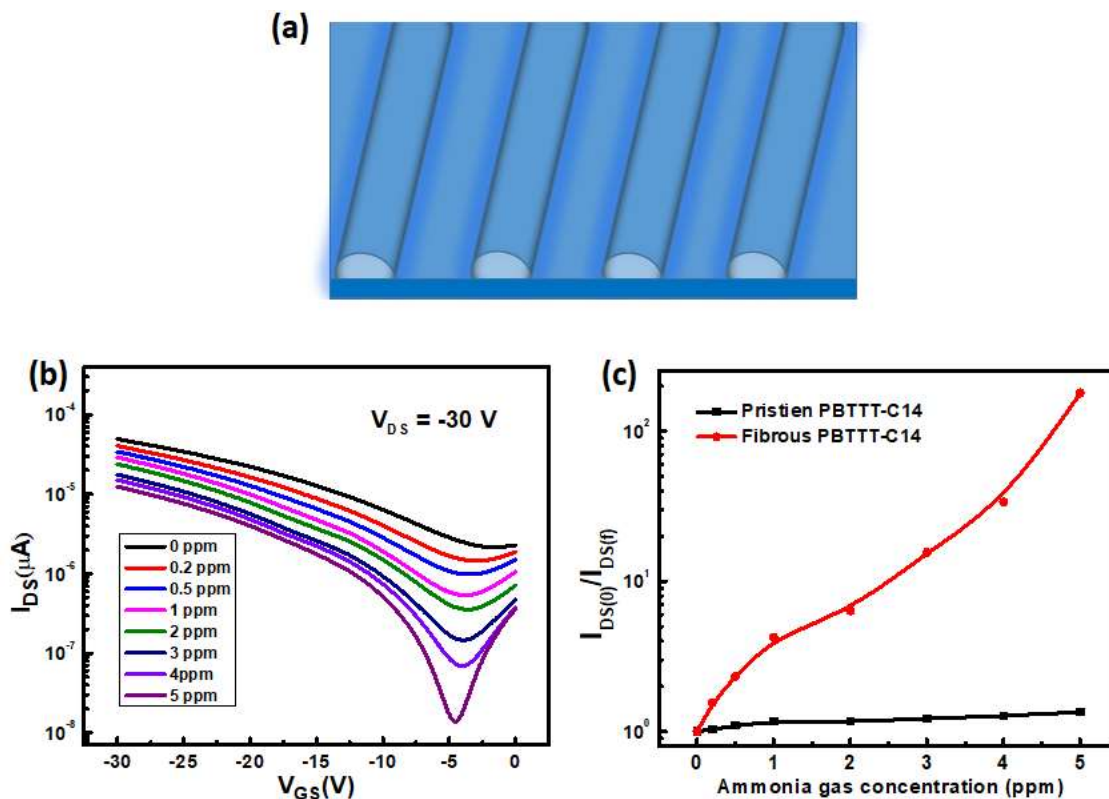


**Fig. 5.8.** (a) Schematic presentation of align nanowires/thin film hybrid channel, (b) variation in OFF current of the OTFT sensor, and (c) corresponding OFF current factor with the  $\text{NH}_3$  concentrations (The data points with black line indicates the OFF current factor of pristine PBTTT-C14 based OTFT device).

When  $\text{NH}_3$  gas enters the conductive channel of the OTFT, it interacts mostly with these nanowires due to their higher effective surface coverage. During this process, the  $\text{NH}_3$  gas diffuses into the fibrillar structure via chemisorption. Since PBTTT-C14 is a p-type semiconductor in which holes serve as the primary charge carriers, therefore as soon reductive  $\text{NH}_3$  interacts, electrons are injected to the nano-wires. This electron injection causes a partial depletion of the channel that results in a large reduction of the  $I_{DS}$  both in accumulation and depletion mode [134, 156].

In the accumulation mode, the variation of  $I_{DS}$  is  $\sim 7$  times larger compared to the pristine film OTFT [156]. As a result, the sensor's response also rises in the same ratio. Simultaneously, due to the deletion of the nano-wires, the sheet resistance of the nano-wires/thin film hybrid channel increases in a larger ratio which reduces the off current (also off current factor) of OTFT in a wide scale that result this OTFT very sensitive in depletion mode operation. Due to the variation of  $NH_3$  concentration from 0 to 5 ppm, the OFF current reduces  $\sim 200$  times which is shown in Figure 5.8(b). Again this variation of the off current of the OTFT, which is presented in term of the 'off current factor', the ratio of the off current of the device under ambient to  $NH_3$  gas ( $I_{D, off}^{amb} / I_{D, off}^{NH_3}$ ), varies quite linearly with  $NH_3$  concentration as illustrated in Fig 5.8(c). It's worth to note that the off current variation of the sensor within the range of 5 ppm  $NH_3$  concentration, is approximately  $\sim 40$  times larger than the ON current variation, indicating its extremely high sensitivity in depletion mode operation.

#### **5.4. Conclusion**

P-type PBTTT-C14 polymer based aligned nanowires/thin film hybrid channel has been used in a top contact bottom gated organic field-effect transistor (OTFT). This OTFT shows an extraordinarily high sensitivity in the low concentration range (0.2 ppm to 5 ppm) of ammonia gas. The fibrillar polymer nano-wires have been grown from the solvent-driven polymer self-assembly, in which a mixed solvent of a good and poor solubility of PBTTT-C14 have been used to prepare the solution. This nano-wires/thin film hybrid film was deposited by the economical and efficient Floating film transfer method (FTM). Various concentrations of  $NH_3$  were exposed on the fibrous polymer-based OTFT channel from 0.2 ppm to 5 ppm to explore the  $NH_3$  sensing behavior of the constructed OTFT. In the accumulation mode operation, the sensor has achieved

~75% response at 5 ppm concentration of NH<sub>3</sub>, which is unusually high in this low concentration range. More interestingly, in the depletion mode operation the variation of drain current is ~100 times higher than its accumulation mode current that results ~200 times off current variation due to the interaction of 5 ppm NH<sub>3</sub> gas. Both in depletion and accumulation mode of operation, variation of channel current is quite linear with NH<sub>3</sub> concentration, which is an important factor for practical application.